

## II. Fundamentals of Free-Radical Polymerization

### Propagation Kinetics in Radical Polymerization Studied via Pulsed Laser Techniques

Michael Buback

**Summary:** Pulsed laser techniques have enormously improved the quality by which rate coefficients of radical polymerization may be determined. The specific and most important feature of the various types of pulsed laser techniques consists in the almost instantaneous production of a significant radical concentration and in the ease by which radical concentration may be controlled by applying further laser pulses at pre-selected delay times. The pulsed laser polymerization – size exclusion chromatography (PLP-SEC) experiment is extremely valuable for the determination of reliable propagation rate coefficients,  $k_p$ . The present article briefly reviews recent results from PLP-SEC studies directed toward the solvent dependence of  $k_p$  in aqueous systems, into  $k_p$  in copolymerization reactions, and into measurements of propagation rate coefficients in systems containing two types of radicals, as is the case with acrylates, where secondary chain-end radicals may undergo 1,5-H shift reactions (backbiting steps) to produce tertiary midchain radicals. By a propagation step, the tertiary radicals are transformed back to secondary ones.

**Keywords:** acrylates; backbiting; methacrylates; propagation kinetics; pulsed laser polymerization

### Introduction

By applying pulsed laser polymerization (PLP) techniques,<sup>[1,2]</sup> the quality of measuring individual rate coefficients of free-radical polymerization has enormously improved. Accurate such rate coefficients are required for a multitude of purposes: (i) They are essential for providing the basis for the fundamental mechanistic understanding of radical polymerizations. (ii) They allow for testing and applying physicochemical rate theory, for comparison with quantum-chemical estimates, and for polymer reaction engineering purposes, in particular for modeling monomer conversion vs. time profiles and polymer properties. (iii) Rate coefficients from PLP are

particularly suitable for applications in controlled/living polymerizations, as the radical size distribution in laser single pulse experiments resembles the one in systems with reversible deactivation. The essential advantage of kinetic analyses via PLP methods consists in the potential of almost instantaneously producing a significant amount of small radicals, by photo-dissociation of suitable initiators, and of the size of growing radicals being proportional to the time  $t$  after applying the laser pulse, unless chain-transfer processes come into play.

Monomer conversion induced by a laser single pulse (SP) may be measured with a time resolution of microseconds via online near infrared (NIR) spectroscopy by the SP-PLP-NIR technique which yields the ratio of propagation to termination rate coefficients,  $k_p/k_t$ .<sup>[3]</sup> By this method, a pointwise probing of  $k_p/k_t$  may be carried out over a wide range of monomer conversion at constant temperature and pressure.<sup>[2]</sup>

Institut für Physikalische Chemie, Georg-August-Universität Göttingen, Tammannstr. 6, D-37077 Göttingen, Germany  
Fax: +49 551 393144; E-mail: mbuback@gwdg.de

More recently, single pulse initiation has been applied in conjunction with time-resolved electron spin resonance (ESR) spectroscopy.<sup>[4,5]</sup> The novel SP-PLP-ESR technique allows for the online detection of the decay in radical concentration after laser pulsing. From a  $c_R$  vs.  $t$  trace, the termination rate coefficient,  $k_t$ , is accessible. As radical size in PLP is linearly increasing with time  $t$  after pulsing, the SP-PLP experiments provide access to  $k_t(i,i)$  values referring to termination of two radicals of (approximately) the same chain length  $i$ . The SP-PLP-ESR results strongly support the validity of the composite model which assumes a stronger decrease of  $k_t(i,i)$  with chain length at smaller  $i$  and a weaker decrease at larger  $i$  after passing the cross-over chain length,  $i_c$ , which separates the short-chain and long-chain regimes.<sup>[6]</sup>

Contrary to the situation with diffusion-controlled  $k_t$  which is affected by chain length, monomer conversion, and by further physical properties of the polymerizing medium, the propagation rate coefficient,  $k_p$ , is generally considered to be chemically controlled and thus to be essentially determined by temperature and pressure. Recent activities of the European Graduate School “Microstructural Control in Radical Polymerization” have addressed detailed aspects of the solvent dependence of  $k_p$ .<sup>[7]</sup> As far as such a dependency exists, it needs to be known for elucidating mechanistic details of radical polymerizations and for the simulation of conversion vs. time curves and of molecular weight distributions as a function of polymerization conditions. In order to clarify whether and why such effects may occur, it seemed worthwhile to investigate systems with strong intermolecular interactions, e.g., hydrogen-bonded monomers in aqueous solution. The present paper briefly reviews the results obtained for methacrylic acid (MAA) in aqueous solution<sup>[8]</sup> and discusses consequences of the novel insights from this MAA work for propagation rate coefficients in less strongly interacting solvents, e.g., in solution and bulk polymerizations of acrylates and methacrylates and in copoly-

merizations<sup>[9]</sup> of members of these two monomer families. Finally, the applicability of the PLP-SEC method toward the kinetic study of propagation in systems with two types of growing radicals will be demonstrated with acrylic acid being taken as an example.

## Experimental Part

Experimental details of the PLP-SEC experiments have been presented elsewhere, e.g., within the studies into MAA in aqueous solution<sup>[8]</sup> and into bulk acrylate–methacrylate polymerizations.<sup>[9]</sup> In what follows, only a very few comments will be given for experiments on MAA (in bulk and in aqueous solution) and on butyl acrylate (representing the studies into acrylates and methacrylates).

Methacrylic acid (Fluka, >98.0%, stabilized with 0.025 wt.% hydroquinone monomethylether) and the photoinitiator DMPA (2,2-dimethoxy-2-phenyl acetophenone, Aldrich, 99%) were used as supplied. The polymerizations were carried out at DMPA concentrations of the order of  $10^{-3}$  mol·L<sup>-1</sup>. Laser pulsing was performed using an excimer laser (LPX 210i, Lambda Physik) operated on the 351 nm (XeF) line. Laser pulse repetition rates were in between 1 and 40 Hz. The monomer solutions were contained in QS165 or QS110 quartz cells (Hellma-Worldwide). MWDs were determined via an aqueous-phase SEC setup consisting of a Waters pump 515 and three Suprema columns (Polymer Standards Service) of particle size 10 μm and pore sizes of 100, 1000 and 3000 Å (positioned in a Waters column heater module), and a differential refractometer (Waters M2410). These experiments were carried out at the Polymer Institute of the Slovak Academy of Sciences (Bratislava) by Dr. I. Lacík and his group. Calibration of the SEC setup was performed with narrowly distributed poly(sodium methacrylate) standards (Polymer Standards Service, PSS) of peak molecular weights between 1250 and 1027000 g·mol<sup>-1</sup>. Data acquisition and

analysis were performed via the WinGPC<sup>®</sup>7.2 software (PSS), which was also used for identification of the position of points of inflection on the MWD (via the maxima of the first derivatives of the MWD curves).

Butyl acrylate (Fluka, 99% purity) was purified by passing through a column filled with inhibitor remover (Aldrich) to remove hydroquinone monomethyl ether, and treated by several freeze-pump and thaw cycles to remove dissolved oxygen. DMPA or MMMP (2-methyl-4-(methylthio)-2-morpholino-propiophenone, Aldrich, 98% purity) have been used as photoinitiators. The SEC analyses were performed at 35 °C with tetrahydrofuran as the eluent on a system composed of a Waters HPLC pump (Model 515), a JASCO AS-2055-plus autosampler, three PSS SDV columns (5  $\mu\text{m}$  particle size;  $10^5$ ,  $10^3$  and  $10^2$  Å pore sizes) and a Waters refractive index detector (Model 2410). The SEC setup was calibrated with polystyrene standards of narrow polydispersity ( $M_p = 410$  to  $2000000 \text{ g} \cdot \text{mol}^{-1}$ , PSS). The primary MWDs data were recalculated according to the principle of universal calibration with the Mark-Houwink parameters for polyBA ( $K = 1.22 \cdot 10^{-2} \text{ mL} \cdot \text{g}^{-1}$ ,  $a = 0.700$ ) and polystyrene ( $K = 1.14 \cdot 10^{-2} \text{ mL} \cdot \text{g}^{-1}$ ,  $a = 0.716$ ).

## Results and Discussion

The aqueous MAA system is of particular interest for studies into solvent effects on  $k_p$ , as PLP-SEC experiments may be carried out over the entire concentration range from one per cent MAA up to bulk MAA polymerization.

The large  $k_p$  data set for methacrylic acid concentrations of  $c_{\text{MAA}} = 1, 2, 3, 5, 10, 15, 20, 30, 40, 45, 60$ , and 100 wt.% and four temperatures from 25 to 80 °C is presented in Ref.<sup>[8]</sup>.

As a representative illustration of the experimental data, MWDs for PLP-SEC studies at 5 and 100 wt.% MAA and 25 °C are presented in Figure 1. The underlying PLP experiments were carried out at a

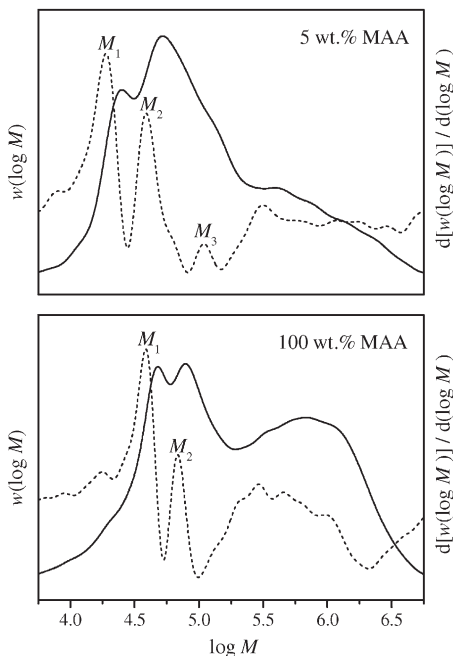


**Figure 1.**

Molecular weight distributions (solid lines) and associated first-derivative curves (dashed lines) of polyMAA obtained by bulk PLP (100 wt.% MAA) and by PLP in dilute aqueous solution (5 wt.% MAA) at 25 °C and a laser repetition rate of 20 Hz.

pulse repetition rate of 20 Hz. Particularly noteworthy is the enormous reduction in  $k_p$  upon increasing MAA concentration. This order-of-magnitude change is illustrated by the  $k_p$  vs.  $c_{\text{MAA}}$  plot for 25 °C in Figure 2.

As has been detailed in Ref.<sup>[8]</sup>, the significant lowering of  $k_p$  with MAA content is essentially, if not entirely, due to a decrease of the Arrhenius pre-exponential factor,  $A(k_p)$ . The activation energy,  $E_A(k_p)$ , on the other hand, appears to be more or less insensitive toward  $c_{\text{MAA}}$ . The pronounced effect may be adequately understood in terms of the transition state theory. As Heuts et al. pointed out,<sup>[10]</sup> the size of  $A(k_p)$  is largely governed by the degree to which the internal rotations of the transition state (TS) for propagation are hindered. This fundamental kinetic effect is associated with the fact that three transitional degrees of freedom are replaced by internal rotational or hindered vibrational

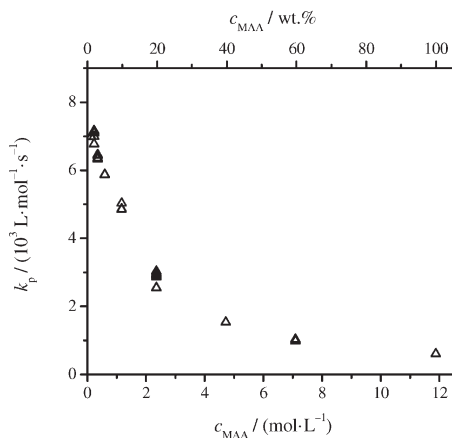


**Figure 2.**

Variation of the propagation rate coefficient,  $k_p$ , of methacrylic acid with MAA concentration in aqueous solution at 25 °C.

degrees of freedom upon formation of the TS structure from a radical and a monomer molecule. In case of severe hindrance of these internal motions, the associated entropy penalty results in a significant lowering of the pre-exponential.

Illustrated in Figure 3 is the TS structure for MAA propagation with this figure being drawn according to a similar type of presentation given by Heuts et al. for the homopolymerization of ethene.<sup>[10]</sup> The

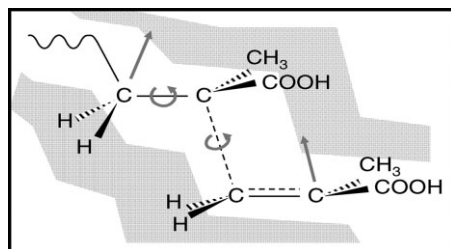


**Figure 3.**

Illustration of the transition state structure for propagation in methacrylic acid polymerization. The grey areas indicate the molecular environment which, in bulk polymerization, consists entirely of MAA molecules and, with MAA propagation in dilute aqueous solution, essentially of water molecules. The arrows indicate internal rotational motion associated with the formation of the TS structure from a radical and a monomer molecule. The figure is adopted from ref.<sup>[7]</sup>

upper left part shows the terminal unit of an MAA macroradical. Given in the lower right part of Figure 3 is the MAA molecule which adds to the macroradical. The dashed line represents the bond which is formed in the TS structure. The arrows indicate the three degrees of hindered internal rotational-type motion which are associated with the formation of the TS. The hindrance of internal rotational mobility may result from intramolecular effects, e.g., the ones induced by substituents at the backbone, and/or from intermolecular effects, e.g., polar or hydrogen bonding interactions. Intermolecular effects play a dominant role in case of MAA propagation because of the strong hydrogen bonds between carboxylic acid moieties. Intramolecular effects should not be responsible for the major changes in hindrance of internal rotational mobility upon varying MAA content, as these interactions do not affect the substitution at the polymeric backbone and thus should not significantly influence the TS structure.

Upon passing from polymerization in dilute aqueous MAA solution to MAA bulk polymerization, the essential change in molecular environment consists in the gradual replacement of water molecules by MAA molecules. Toward higher MAA content, the particularly strong hydrogen-bonded interactions between carboxylic acid groups are becoming dominant. The formation of intermolecular cyclic dimeric COOH structures induces a larger friction than the one associated with the interaction of the TS structure with water molecules.<sup>[8]</sup> That the intermolecular interactions influence  $k_p$  may also be demonstrated by adding sodium hydroxide to the solution of non-ionized MAA. In aqueous solution at 5 wt.% MAA,  $k_p$  is lowered by about one order of magnitude in passing from the non-ionized to the fully ionized monomer.<sup>[7]</sup>

That  $A(k_p)$  is correlated with the hindrance to chain mobility of the transition structure, may also be seen from a comparison of the  $A(k_p)$  values of MAA, methyl methacrylate (MMA) and methyl acrylate (MA) bulk homopolymerizations.<sup>[2,8]</sup>

These  $A(k_p)$  values read:

$$\begin{aligned} 0.38 \cdot 10^6 \text{ L} \cdot \text{mol}^{-1} \cdot \text{s}^{-1} & \quad (\text{MAA}) \\ 0.67 \cdot 10^6 \text{ L} \cdot \text{mol}^{-1} \cdot \text{s}^{-1} & \quad (\text{MAA}) \\ 16.6 \cdot 10^6 \text{ L} \cdot \text{mol}^{-1} \cdot \text{s}^{-1} & \quad (\text{MA}). \end{aligned}$$

With respect to  $A(k_p)$  of MMA, the pre-exponential of MAA is lower by about one order of magnitude because of the hindrance provided by the strong hydrogen bonds. The  $A(k_p)$  value of MA, on the other hand, is significantly higher, which is assigned to the favourable effect on internal rotational mobility of replacing the methyl group at every second carbon atom of the backbone by an  $\alpha$ -hydrogen atom.

The studies into  $k_p$  of MAA in aqueous solution are of general importance in making clear that the propagation rate coefficient may be solvent dependent. The explanation behind the strong effect is a genuine kinetic one, which indicates that such effects may occur with all systems, however, to widely differing extents. The strong solvent effect on  $k_p$  seen in aqueous solution of MAA is due to the significant difference of intermolecular interactions of the TS structure with an environment essentially consisting of water molecules and an environment consisting of MAA molecules. Thus different degrees of friction to internal rotation are experienced which give rise to largely different pre-exponentials,  $A(k_p)$ .

That  $k_p$  has mostly been considered as insensitive toward adding a solvent, is primarily due to the fact that mostly solvents have been investigated which, with respect to polarity, are similar to the monomer. With monomer and solvent having (almost) the same polarity, kinetic theory predicts at best small differences between bulk and solution  $A(k_p)$ . It needs to be kept in mind that bulk polymerization may be considered as a solution polymerization with the monomer acting as the solvent. An immediate consequence of this latter insight is that  $k_p$  should not depend on the degree of conversion in bulk polymerizations, as the molecular environment of the TS structure remains the same through-

out the polymerization to higher conversion. Only under conditions of significant coil overlap and in case of monomer transport running under diffusion control, bulk  $k_p$  may change during the course of a polymerization.

This insensitivity of (bulk polymerization)  $k_p$  toward the degree of monomer conversion must not hold in solution polymerizations, as has been demonstrated for MAA polymerizations in aqueous solution,<sup>[11]</sup> where  $k_p$  was observed to increase toward higher degrees of monomer conversion. This effect may also be adequately understood on the basis of the genuine kinetic argument that it is the friction experienced by the TS structure which controls  $A(k_p)$ . During MAA solution polymerization, MAA molecules in the vicinity of the TS state structure, e.g., within the coiled macroradical, are replaced by water molecules thus lowering the friction to internal rotation and enhancing  $A(k_p)$ . It should be noted that this change occurs at constant overall density of -COOH moieties. Polymeric MAA segments, however, are not affecting the molecular environment at the radical site, which is essentially given by the ratio of MAA monomer to water molecules.

The fundamental insight into the dependence of  $A(k_p)$  on inter- and intramolecular interactions affecting the size of  $k_p$ , turns out to be helpful for the better understanding of other types of unexpected  $k_p$  behavior. Two examples will be given in the subsequent text. They refer to the variation of  $k_p$  with alkyl ester size in the acrylate and methacrylate monomer families and to propagation in acrylate-methacrylate copolymerizations.

Plotted in Figure 4 is the variation with the size of the alkyl group of  $k_p$  within the acrylate family for both bulk polymerization (triangles) and solution-in-toluene polymerization (circles). Ester size increases from left to right with methyl acrylate (MA) and dodecyl acrylate (DA) being the smallest and largest family members, respectively. The solution data for 20 °C have been determined by the Paris group.<sup>[12]</sup> The

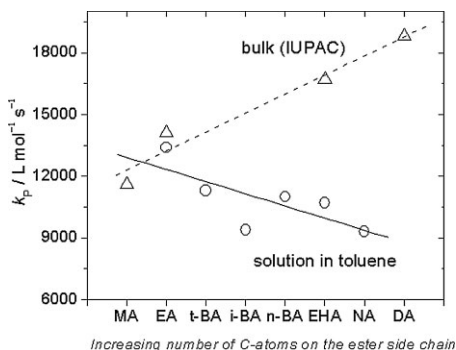


**Figure 4.**

Comparison of propagation rate coefficients for a series of alkyl acrylates in bulk polymerizations (triangles) and in solution polymerizations (1.5 to 4.7 molar) in toluene (circles) at 20 °C. The solution data are from Ref.<sup>[12]</sup>. The acronyms refer to acrylates with methyl (MA), ethyl (EA), *tert*-butyl (t-BA), *iso*-butyl (i-BA), butyl (n-BA), 2-ethylhexyl (EHA), nonyl (NA) and dodecyl (DA) ester groups.

bulk data are from ref.<sup>[2]</sup>. Interestingly, bulk  $k_p$  is clearly enhanced toward increasing alkyl ester size, whereas the solution-in-toluene  $k_p$  values exhibit some lowering of  $k_p$  toward larger size of the alkyl group. It should be noted that bulk  $k_p$  increases with ester size also within the methacrylate family. The  $k_p$  value for MMA bulk polymerization is clearly below the associated value for dodecyl methacrylate.<sup>[2]</sup>

The different type of  $k_p$  behavior, in bulk and in toluene solution, has induced several activities within both the Paris group and our group, which were directed toward resolving the apparent discrepancy. The new insight into the impact of intermolecular interactions on  $A(k_p)$  may account for the discrepancies and even suggests that the  $k_p$  values for bulk and solution (Figure 4) are both reasonable. The increase in bulk  $k_p$  in passing from MA to DA may be understood as resulting from the enhanced shielding of the polar groups of the TS structure by the longer non-polar alkyl groups. As a consequence, the dipolar interactions are becoming weaker in passing from MA to DA. This change is accompanied by less friction and thus by an increase in  $k_p$ . Within the solution experiments, the molecular environment varies to

a much weaker extent, as toluene acts as the solvent with all the acrylates under investigation. Thus no major change in friction of rotational mobility within the TS is expected. The weak decrease in  $k_p$  that seems to occur toward larger size of the alkyl group may be assigned to enhanced shielding of the radical site.

The assignment of changes in  $k_p$  to internal rotational mobility in the TS may also explain the trend revealed by careful studies into the solvent dependence of MMA and *iso*-bornyl methacrylate  $k_p$ .<sup>[13]</sup> relative to bulk  $k_p$ , the solution  $k_p$  value increases in solvents with the molar volume exceeding the one of the pure monomer and vice versa. Larger solvent molecules afford for more rotational freedom than do smaller solvent molecules, as the latter species may better fill voids between particles.

Copolymerization  $k_p$  behaviour shows some peculiarities which are also easier understood via the entropy penalty argument for  $A(k_p)$ . Alkyl acrylate – alkyl methacrylate copolymerizations have been studied at 1000 bar and temperatures from 22 to 40 °C.<sup>[14,15]</sup> High-pressure measurements were performed, as such data were required for deducing termination rate coefficients from experimentally determined high-pressure coupled rate coefficients,  $k_{p, \text{copo}}/k_{t, \text{copo}}$ . The liquid monomers are not overly compressible. Thus, the mechanistic information deduced from the high-pressure experiments should also hold for ambient-pressure conditions. Given in Figure 5 is the copolymerization diagram of four acrylate–methacrylate pairs of monomers. The systems differ in that a small acrylate, methyl acrylate (MA), is combined with a small methacrylate (MMA) and a large methacrylate (DMA) to yield the systems: MA–MMA and MA–DMA, respectively. With the other two systems, dodecyl acrylate (DA) is combined with a small and a large methacrylate, MMA and DMA, respectively, to yield the copolymerization systems DA–MMA and DA–DMA.

Interestingly, the correlation of monomer mixture and copolymer compositions



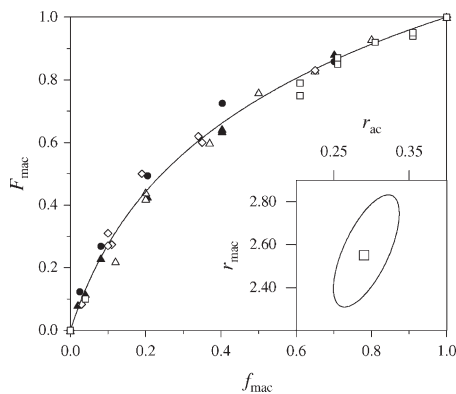


**Figure 5.**

Copolymerization diagram for several acrylate-methacrylate systems at 1000 bar: DA-DMA (40 °C; squares), MA-DMA (40 °C; diamonds), DA-MMA (23 °C; full triangles, 40 °C; open triangles), and MA-MMA (23 °C; full circles). Given in the inset to the figure is the 95% confidence interval for the reactivity ratios,  $r_{\text{ac}}$  and  $r_{\text{mac}}$ . The figure is from Ref.<sup>[15]</sup>.

for the four copolymerization systems may be adequately represented by one single pair of acrylate and methacrylate reactivity ratios,  $r_{\text{ac}}$  and  $r_{\text{mac}}$ . This result appears surprising, as it has become clear that the penultimate unit effect (PUE) model has to be used for representation of copolymerization kinetics. The results in Figure 4 have shown that the size of the alkyl chain length clearly affects  $k_p$ . Therefore, one would expect the reactivity ratios to also vary with ester size.

In terms of the PUE model, four reactivity ratios,  $r_{ij}$ , and two radical reactivity ratios,  $s_i$  and  $s_j$ , need to be considered. For the copolymerization of monomers 1 and 2 the PUE parameters read as follows:

$$r_{11} = \frac{k_{p111}}{k_{p112}} \quad r_{21} = \frac{k_{p211}}{k_{p212}}$$

$$r_{22} = \frac{k_{p222}}{k_{p221}} \quad r_{12} = \frac{k_{p122}}{k_{p121}}$$

$$s_1 = \frac{k_{p211}}{k_{p111}} \quad s_2 = \frac{k_{p122}}{k_{p222}}$$

The individual propagation rate coefficients,  $k_{pijk}$ , refer to the addition of monomer  $k$  to a radical chain-end with a terminal

unit that results from addition of monomer  $j$  and a penultimate unit from adding monomer  $i$  in the preceding step. The data in Figure 5 suggests that, to a good approximation,  $r_{11} = r_{21}$  and  $r_{22} = r_{12}$ , which reduces the total of four reactivity ratios to the two reactivity ratios,  $r_1$  and  $r_2$ :

$$r_1 = r_{11} = r_{21}$$

and

$$r_2 = r_{22} = r_{12}$$

which afford for a satisfactory correlation of copolymer composition with monomer mixture composition. The reason, why this simplification holds in most cases, probably is that, e.g., both  $r_{11} = k_{p111}/k_{p112}$  and  $r_{21} = k_{p211}/k_{p212}$  are ratios of PUE propagation rate coefficients referring to radicals with identical terminal and penultimate unit. Obviously, the ratioing procedure eliminates most of the impact of the penultimate unit on the rate coefficients. The same argument may be used to explain why  $r_{22}$  is close to  $r_{12}$ .

The second finding from Figure 5 is that each reactivity ratio,  $r_{\text{ac}}$  and  $r_{\text{mac}}$ , is insensitive toward the type of monomer that is added to a particular chain-end, which says that, e.g.,  $r_{\text{MA}}$  is the same in MA-MMA and MA-DMA copolymerization. This is equivalent to stating that  $k_{p\text{MA,MA,MA}}/k_{p\text{MA,MA,MMA}}$  is very close or even identical to  $k_{p\text{MA,MA,MA}}/k_{p\text{MA,MA,DMA}}$  which results in  $k_{p\text{MA,MA,MMA}} \approx k_{p\text{MA,MA,DMA}}$ . That these two rate coefficients should indeed be close to each other may be understood by inspection of Figure 3. The region of the TS structure which determines the extent of hindrance to internal rotation encompasses the radical chain-end (probably including the penultimate segment) and the  $\text{CH}_2=\text{C}$  part of the monomer. The alkyl ester group is probably too far away from this kinetically relevant area as to significantly affect the PUE rate coefficient  $k_{p\text{MA,MA,mac}}$  in which “mac” refers to an arbitrary alkyl methacrylate. Because of the relevant positions being identical,  $k_{p\text{MA,MA,MMA}}$  and  $k_{p\text{MA,MA,DMA}}$  will not be significantly different. The same type of

argument explains why the  $r_{\text{mac}}$  values are insensitive toward the type of alkyl acrylate – alkyl methacrylate system.

The almost perfect agreement in composition behaviour of the four acrylate–methacrylate systems in Figure 5 may suggest that also the propagation behaviour of these systems is very similar. The results reported for the copolymerization propagation rate coefficient,<sup>[15]</sup>  $k_{\text{p, copo}}$ , of MA–MMA and MA–DMA at 23 °C and 1000 bar are plotted in Figure 6. The full lines represent fits to the implicit penultimate unit (IPUE) model, whereas the dotted lines are calculated from the simple terminal unit model assuming the reactivity ratios from composition analysis,  $r_{\text{ac}} = 0.29$  and  $r_{\text{mac}} = 2.55$ , to hold. The very remarkable observation from Figure 6 is that the terminal model affords for an adequate fit of the measured  $k_{\text{p, copo}}$  data for the two MA-containing copolymerization systems. Even more surprising is the excellent quality of the fit in case that the alkyl ester size is dissimilar for the acrylate and the methacrylate monomer. For this MA–DMA system, the terminal model with one pair of reactivity ratios is capable of simultaneously representing copolymer

composition and copolymer propagation behaviour.

The behaviour of MA–DMA raised interest in testing whether also with the complementary system, DA–MMA, the variation with  $f_{\text{mac}}$  of composition and propagation may be fitted by the terminal model with a single pair of reactivity ratios. The  $k_{\text{p, copo}}$  data for DA–MMA from Ref.<sup>[15]</sup> show a completely different picture (Figure 7). The terminal model with  $r_{\text{ac}} = 0.29$  and  $r_{\text{mac}} = 2.55$  (dotted line) completely fails to reproduce the experimental data, but also the IPUE model (full line) is not overly satisfactory. The best representation of  $k_{\text{p, copo}}$  is achieved by fitting the data to a terminal model expression that is applied to the  $k_{\text{p, copo}}$  data alone (dashed line). The quality of the resulting fit is, however, also not impressive. A further and substantial disadvantage of using such a (dashed line) fit of  $k_{\text{p, copo}}$  results from the fact that this procedure yields a second pair of  $r_{\text{ac}}$  and  $r_{\text{mac}}$  values ( $r_{\text{ac}} = 0.30$ ,  $r_{\text{mac}} = 0.64$ ) which largely differs from the corresponding  $r_{\text{ac}}$  –  $r_{\text{mac}}$  pair from composition analysis (see Figure 5) and would, incorrectly, suggest azeotropic

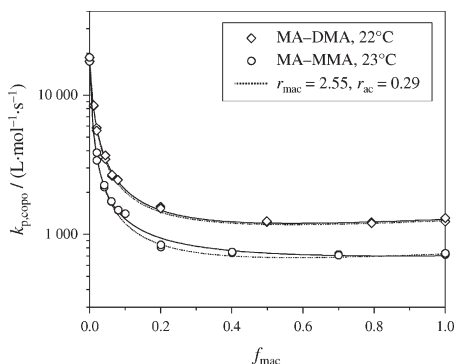


**Figure 6.**

Copolymerization propagation rate coefficients,  $k_{\text{p, copo}}$ , as a function of  $f_{\text{mac}}$ , the methacrylate mole fraction of the monomer mixture, at 1000 bar. The dotted line is from terminal model fitting with  $r_{\text{mac}} = 2.55$  and  $r_{\text{ac}} = 0.29$ , the full line from IPUE modeling. The figure is from ref.<sup>[15]</sup>.

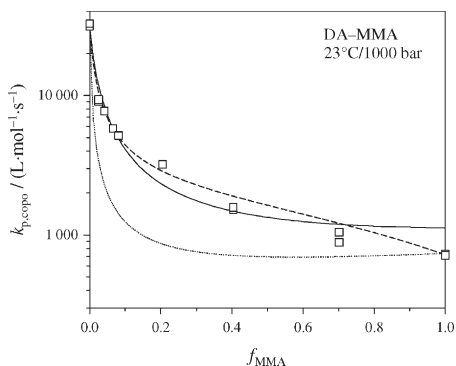


**Figure 7.**

Copolymerization propagation rate coefficient,  $k_{\text{p, copo}}$ , for the DA–MMA system at 23 °C and 1000 bar plotted as a function of the methacrylate mole fraction of the monomer mixture,  $f_{\text{mac}}$ . The dotted line is from terminal model fitting with  $r_{\text{mac}} = 2.55$  and  $r_{\text{ac}} = 0.29$ , the full line from IPUE modeling, and the dashed line from terminal model fitting only of  $k_{\text{p, copo}}$ , which results in the reactivity ratios  $r_{\text{mac}} = 0.64$  and  $r_{\text{ac}} = 0.30$ . The figure is from ref.<sup>[15]</sup>



behaviour for the DA-MMA system. The two sets of reactivity ratios with DA-MMA demonstrate that penultimate unit effects are operative.

In order to keep the number of adjustable parameters low, a simplified IPUE model has been used, which adopts the reactivity ratio data from composition analysis and further assumes the product of the two radical reactivity ratios to be unity:  $s_{ac} \cdot s_{mac} = 1$  or  $s_{ac} = s_{mac}^{-1}$ . Thus  $s_{ac}$  is the single parameter to be deduced from simultaneously fitting the experimental composition and  $k_{p, copo}$  data. As is to be expected from Figure 6, the fitting procedure for the MA-DMA system yields:  $s_{MA} = 0.99$  and  $s_{DMA} = 1.01$ , which reflects the almost perfect terminal model behaviour. For the complementary system, DA-MMA, the radical reactivity ratios are obtained from the fitting procedure to be:  $s_{DA} = 0.09$  and  $s_{MMA} = 11.32$ . The large deviations from unity suggest that it may even be insufficient to consider terminal and penultimate units and that penultimate segments should be included too.

As the enormous difference in propagation behaviour of the MA-DMA and DA-MMA systems is not easily understood, the above-mentioned hindrance-to-internal mobility arguments have been applied.<sup>[15]</sup> Two contributions to hindrance of rotational mobility may be distinguished: (i) an intermolecular mobility term, *interMT*, associated with the effective shielding of dipolar intermolecular interactions by large alkyl ester groups, and (ii) an intramolecular mobility term, *intraMT*, associated with the type of penultimate unit on the macroradical. Replacing a methacrylate penultimate segment by an acrylate segment has a favourable effect on chain-end mobility and vice versa. The *intraMT* and *interMT* contributions are collated in Table 1 for the four copolymerizations.

The *intraMT* lowers  $s_{ac} = k_{p, mac, ac, ac} / k_{p, ac, ac, ac}$  to values below unity, as the methacrylate segment reduces mobility as compared to the action of an acrylate unit. Along the same argument, the *intraMT*

**Table 1.**

Intermolecular and intramolecular mobility terms affecting the acrylate and methacrylate radical reactivity ratios,  $s_{ac}$  and  $s_{mac}$ , respectively.

		$s_{ac} = k_{p, mac, ac, ac} / k_{p, ac, ac, ac}$		$s_{mac} = k_{p, ac, mac, mac} / k_{p, mac, mac, mac}$	
		<i>interMT</i>	<i>intraMT</i>	<i>interMT</i>	<i>intraMT</i>
MA-MMA	1	<1	1	>1	
MA-DMA	>1	<1	<1	>1	
DA-MMA	<1	<1	>1	>1	
DA-DMA	1	<1	1	>1	

increases  $s_{mac}$  to values above unity. The *interMT* is assumed to play no major role in systems where the acrylate and methacrylate segments have the same alkyl ester group. This situation is reflected in Table 1 by the entry *interMT* = 1, e.g., for MA-MMA and DA-DMA. With MA-DMA, the *interMT* for  $s_{MA}$  exceeds unity because of the larger shielding capacity of the dodecyl moiety of the methacrylate. According to this argument,  $s_{DMA}$  is diminished to values below unity. The reverse is true for DA-MMA, where the *interMT* of  $s_{DA}$  is below unity and the *interMT* of  $s_{MMA}$  is above unity.

Inspection of the entries in Table 1 reveals that the arguments related to hindrance of internal rotational motion in the TS structure provide an adequate explanation for the significant differences of the  $k_{p, copo}$  behaviour for the MA-DMA and DA-MMA copolymerizations. With the MA-DMA system, the individual contributions to both  $s_{ac}$  and to  $s_{mac}$  are opposite to each other, in that one contribution is below, the other above unity (see Table 1). That the resulting radical reactivity ratios with MA-DMA are close to unity indicates that the intermolecular and intramolecular mobility terms are approximately similar in (absolute) size. With the DA-MMA system, the intermolecular and intramolecular mobility terms for each radical reactivity ratio point into the same direction. This leads to  $s_{ac}$  being well below and to  $s_{mac}$  being well above unity.

At present, it is not clear whether this novel kinetic understanding of  $k_{p, copo}$  requi-

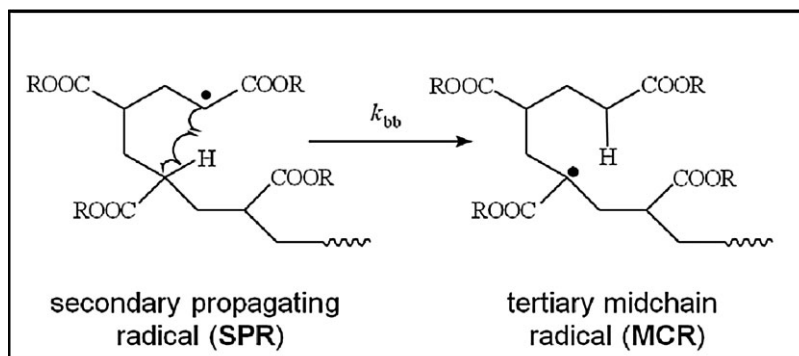
res a modified general treatment, e.g., one which takes pen-penultimate effects into account. Because of the large size of the dodecyl moiety, which clearly exceeds the length of two repeat units, it is understandable that in both DA and DMA several chain segments may be shielded by one side group.

It is beyond the scope of this brief review-type article to address the specific aspects of PLP-SEC analyses into acrylates in any detail. The additional problems with these monomers are due to the occurrence of backbiting processes, which transform a secondary propagating (chain-end) radical, SPR, into a tertiary midchain radical, MCR, via a 1,5-hydrogen shift reaction (see Scheme 1). The addition of a monomer radical to the so-produced MCR is by at least two orders of magnitude slower than the addition rate of monomer to an SPR. The backbiting step thus effectively disturbs the cutting action of a subsequent laser pulse, by which, in the absence of backbiting, the characteristic chain length of polymeric material is controlled by the laser pulse repetition rate (under otherwise suitably selected PLP conditions). The interference of backbiting does not invalidate the results of the acrylate–methacrylate PLP-SEC experiments presented above, as the  $k_{p, \text{copo}}$  measurements were carried out at ambient temperature,

where the impact of backbiting is not that important. The above  $k_{p, \text{copo}}$  data for acrylate-containing systems thus refer to propagation of SPRs.

Toward higher temperatures, the statistically occurring backbiting process contributes to an increasing extent, which leads to a significant broadening of the experimental PLP-SEC traces and thus poses problems for the determination of  $k_p$ . As was demonstrated in the pioneering simulation study by the Paris group, even under conditions where backbiting and laser-induced stopping of propagation occur at similar rates, PLP-SEC experiments may provide kinetic information when laser pulsing is performed at several widely different pulse repetition rates.<sup>[16]</sup>

The first experimental results on this matter have been provided by our group on acrylic acid polymerization in aqueous phase.<sup>[17]</sup> A detailed study via the novel frequency-tuned PLP-SEC (ft-PLP-SEC) method has been carried out on butyl acrylate.<sup>[18]</sup> A brief account of ft-PLP-SEC is presented in Figure 8, where PLP-SEC results from Ref.<sup>[17]</sup> on 1.35 M acrylic acid in aqueous solution at pulse repetition rates between 10 and 100 Hz are shown. The SEC traces were analyzed in the usual way by deducing an apparent  $k_p$  value,  $k_p^{\text{app}}$ , from the degree of polymerization at the first point of inflection on the MWD.



**Scheme 1.**

Backbiting reaction.

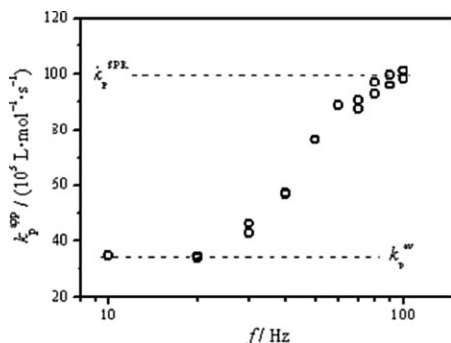


**Figure 8.**

Variation of the apparent propagation rate coefficient (see text) with the applied laser pulse repetition rate,  $f$ , for PLP-SEC experiments on 1.35 M acrylic acid in aqueous solution at 6 °C. The data is from Ref. [17].

At the highest pulse repetition rates,  $k_p^{\text{app}}$  approaches  $k_p$  of secondary (SPR) chain-end radicals for the simple reason that the laser cutting action is too fast as to allow for a significant extent of backbiting. Toward lower pulse repetition frequency,  $f$ , backbiting increasingly comes into play and a significant fraction of radicals undergoes backbiting during the time interval between two successive laser pulses. As is detailed in Ref. [18], the backbiting rate coefficient may be obtained from the  $f$  value at which the characteristic degree of polymerization associated with laser-induced stopping of the chain growth can no longer be observed. From this typical value on,  $k_p^{\text{app}}$  clearly decreases toward lower pulse repetition frequencies. At rather low  $f$  values,  $k_p^{\text{app}}$  approaches another plateau value,  $k_p^{\text{av}}$ , at conditions where the cycle of (initial) growth of the SPRs, of backbiting to form midchain radicals (MCRs), of formation of SPRs by a growth reaction of the MCRs, and subsequent growth of re-formed SPRs occurs so frequently that laser pulsing can act as a cutting tool for this periodic overall process. In conjunction with  $k_p^{\text{SPR}}$  and the backbiting rate coefficient,  $k_{\text{bb}}$ , which two quantities are obtained within the same experimental series, but at higher  $f$ , the  $k_p^{\text{av}}$  plateau value allows for deducing the rate coefficient of propagation for a tertiary midchain radical,  $k_p^{\text{MCR}}$ .

## Conclusion

Accurate propagation rate coefficients,  $k_p$ , are accessible from pulsed laser polymerization – size exclusion chromatography (PLP-SEC) experiments. Recent progress in this field allows for studies into  $k_p$  of systems with strong intermolecular interactions, such as are occurring with (meth)acrylic acid in aqueous solution. The unusually large changes of  $k_p$  as a function of MAA content are adequately understood on the basis of fundamental rate theory, in particular, by the well established insight that the hindrance to internal rotational motion essentially determines the size of the Arrhenius pre-exponential factor. This knowledge allows for a satisfactory interpretation also of other effects, which were not fully understood so far, e.g., the variation with alkyl ester size of  $k_p$  within the acrylate and methacrylate families or the copolymerization  $k_p$  behavior of acrylate–methacrylate systems. Recent developments in PLP-SEC allow for the measurement of rate coefficients also for systems in which different types of growing radicals, such as secondary chain-end and tertiary midchain radicals, are present. For the latter systems, also the backbiting rate coefficient for the 1,5-hydrogen shift reaction, by which a secondary radical is transformed into a tertiary one, may be deduced from frequency-tuned PLP-SEC in which a wide range of laser pulse repetition rates is applied.

**Acknowledgements:** Financial support by the *Deutsche Forschungsgemeinschaft* within the frame of the European Graduate School “Microstructural Control in Free-Radical Polymerization” is gratefully acknowledged as is support by *Jens Schrooten* and *Durga Prasad Saggi* in finalizing the manuscript.

[1] O. F. Olaj, I. Bitai, F. Hinkelmann, *Makromol. Chem.* **1987**, 188, 1689.

[2] S. Beuermann, M. Buback, *Prog. Polym. Sci.* **2002**, 27, 191.

[3] M. Buback, H. Hippler, J. Schweer, H. P. Vögele, *Makromol. Chem., Rapid Commun.* **1986**, 7, 261.

- [4] M. Buback, M. Egorov, T. Junkers, E. Panchenko, *Macromol. Rapid Commun.* **2004**, 25, 1004.
- [5] M. Buback, E. Müller, G. T. Russell, *J. Phys. Chem. A* **2006**, 110, 3222.
- [6] G. B. Smith, G. T. Russell, J. P. A. Heuts, *Macromol. Theory Simul.* **2003**, 12, 299.
- [7] S. Beuermann, M. Buback, P. Hesse, S. Kukučková, I. Lacik, *Macromol. Symp.* **2007**, 248, 23.
- [8] S. Beuermann, M. Buback, P. Hesse, I. Lacik, *Macromolecules* **2006**, 39, 184.
- [9] M. Buback, E. Müller, *Macromol. Chem. Phys.* **2007**, 208, 581.
- [10] J. P. A. Heuts, R. G. Gilbert, L. Radom, *Macromolecules* **1995**, 28, 8771.
- [11] S. Beuermann, M. Buback, P. Hesse, S. Kukučková, I. Lacik, *Macromol. Symp.* **2007**, 248, 41.
- [12] L. Couvreur, G. Piteau, P. Castignolles, M. Tonge, B. Coutin, B. Charleux, J.-P. Vairon, *Macromol. Symp.* **2001**, 174, 197.
- [13] S. Beuermann, N. Garcia, *Macromolecules* **2004**, 37, 3018.
- [14] M. Buback, A. Feldermann, C. Barner-Kowollik, I. Lacik, *Macromolecules* **2001**, 34, 5439.
- [15] M. Buback, E. Müller, *Macromol. Chem. Phys.* **2007**, 208, 581.
- [16] A. Nikitin, P. Castignolles, B. Charleux, J.-P. Vairon, *Macromol. Rapid Commun.* **2003**, 24, 778.
- [17] M. Buback, P. Hesse, I. Lacik, *Macromol. Rapid Commun.* **2007**, 28, **2049**.
- [18] A. N. Nikitin, R. A. Hutchinson, M. Buback, P. Hesse, *Macromolecules* **2007**, 40, 8631.